
This is an electronic reprint of the original article.
This reprint may differ from the original in pagination and typographic detail.

Author(s): Pashkin, Yu. A. & Li, T. F. & Pekola, Jukka & Astafiev, O. & Knyazev, D. A. & Hoehne, F. & Im, H. & Nakamura, Y. & Tsai, J. S.

Title: Detection of mechanical resonance of a single-electron transistor by direct current

Year: 2010

Version: Final published version

Please cite the original version:

Pashkin, Yu. A. & Li, T. F. & Pekola, Jukka & Astafiev, O. & Knyazev, D. A. & Hoehne, F. & Im, H. & Nakamura, Y. & Tsai, J. S. 2010. Detection of mechanical resonance of a single-electron transistor by direct current. Applied Physics Letters. Volume 96, Issue 26. P. 263513/1-3. ISSN 0003-6951 (printed). DOI: 10.1063/1.3455880.

Rights: © 2010 American Institute of Physics. This article may be downloaded for personal use only. Any other use requires prior permission of the author and the American Institute of Physics. The following article appeared in Applied Physics Letters and may be found at <http://scitation.aip.org/content/aip/journal/apl/96/26/10.1063/1.3455880>

All material supplied via Aaltodoc is protected by copyright and other intellectual property rights, and duplication or sale of all or part of any of the repository collections is not permitted, except that material may be duplicated by you for your research use or educational purposes in electronic or print form. You must obtain permission for any other use. Electronic or print copies may not be offered, whether for sale or otherwise to anyone who is not an authorised user.

Detection of mechanical resonance of a single-electron transistor by direct current

Yu. A. Pashkin, T. F. Li, J. P. Pekola, O. Astafiev, D. A. Knyazev, F. Hoehne, H. Im, Y. Nakamura, and J. S. Tsai

Citation: [Applied Physics Letters](#) **96**, 263513 (2010); doi: 10.1063/1.3455880

View online: <http://dx.doi.org/10.1063/1.3455880>

View Table of Contents: <http://scitation.aip.org/content/aip/journal/apl/96/26?ver=pdfcov>

Published by the [AIP Publishing](#)

Articles you may be interested in

[Fabrication of nanogapped single-electron transistors for transport studies of individual single-molecule magnets](#)

[J. Appl. Phys.](#) **101**, 09E102 (2007); 10.1063/1.2671613

[Electric-field-dependent spectroscopy of charge motion using a single-electron transistor](#)

[Appl. Phys. Lett.](#) **88**, 213118 (2006); 10.1063/1.2207557

[Superconducting single-electron transistor coupled to a locally tunable electromagnetic environment](#)

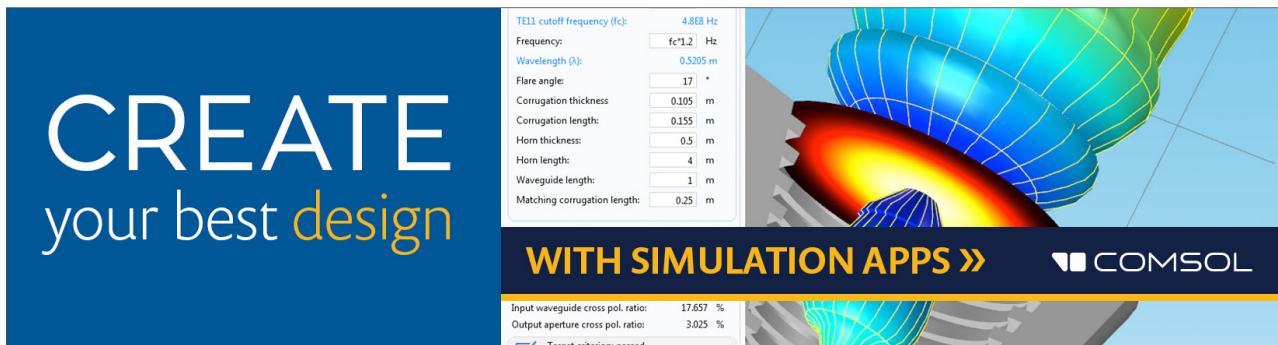
[Appl. Phys. Lett.](#) **81**, 4976 (2002); 10.1063/1.1530731

[Single-electron capacitance spectroscopy of vertical quantum dots using a single-electron transistor](#)

[Appl. Phys. Lett.](#) **74**, 555 (1999); 10.1063/1.123143

[Metallic resistively coupled single-electron transistor](#)

[Appl. Phys. Lett.](#) **74**, 132 (1999); 10.1063/1.122973

The advertisement features a dark blue background on the left with the text 'CREATE your best design' in white and yellow. On the right, there is a 3D simulation of a horn-shaped antenna structure with a color gradient from blue to red. A control panel is overlaid on the simulation, showing various parameters for a TE11 cutoff frequency. The parameters include Frequency (4.868 Hz), Wavelength (0.5205 m), Flare angle (17 degrees), Corrugation thickness (0.105 m), Corrugation length (0.155 m), Horn thickness (0.5 m), Horn length (4 m), Waveguide length (1 m), and Matching corrugation length (0.25 m). Below the control panel, the text 'WITH SIMULATION APPS >>' is displayed in yellow, followed by the COMSOL logo. At the bottom, there are two rows of data: 'Input waveguide cross pol. ratio: 17.657 %' and 'Output aperture cross pol. ratio: 3.025 %', with a checked box for 'Target criterion: passed'.

Detection of mechanical resonance of a single-electron transistor by direct current

Yu. A. Pashkin,^{1,a)} T. F. Li,^{1,2} J. P. Pekola,³ O. Astafiev,¹ D. A. Knyazev,⁴ F. Hoehne,^{1,5} H. Im,^{1,6} Y. Nakamura,¹ and J. S. Tsai¹

¹NEC Nano Electronics Research Laboratories and RIKEN Advanced Science Institute, Tsukuba, Ibaraki 305-8501, Japan

²Institute of Microelectronics, Tsinghua University, Beijing 100084, People's Republic of China

³Low Temperature Laboratory, Aalto University School of Science and Technology, P.O. Box 13500, FI-00076 Aalto, Finland

⁴P. N. Lebedev Physical Institute, Russian Academy of Sciences, Moscow 119991, Russia

⁵Walter Schottky Institut, Technische Universität München, Am Coulombwall 3, 85748 Garching, Germany

⁶Department of Semiconductor Science, Dongguk University, Phil-Dong, Seoul 100-715, Republic of Korea

(Received 18 February 2010; accepted 28 May 2010; published online 1 July 2010)

We have suspended an Al based single-electron transistor (SET) whose island can resonate freely between the source and drain leads forming the clamps. In addition to the regular side gate, a bottom gate with a larger capacitance to the SET island is placed underneath to increase the SET coupling to mechanical motion. The device can be considered as a doubly clamped Al beam that can transduce mechanical vibrations into variations in the SET current. Our simulations based on the orthodox model, with the SET parameters estimated from the experiment, reproduce the observed transport characteristics in detail. © 2010 American Institute of Physics. [doi:10.1063/1.3455880]

Nanomechanical resonators, usually doubly clamped beams or cantilevers, offer rich physics as well as a wide range of applications.^{1,2} In order to do experiments on them, one needs a detector, called a transducer, coupled to the resonator, which converts mechanical displacement into an electrical signal. A number of techniques have been applied to measure mechanical motion at the micro and nanoscales. For the past decade in the quest for higher sensitivity and speed, the dimensions of the resonators were scaled down, pushing their resonance frequency to above 1 GHz.³ At the same time the requirements to the transducers become more stringent in terms of sensitivity to the mechanical displacement, thus narrowing the choice of possible detectors. Among various detection techniques described elsewhere,⁴ a single-electron transistor (SET) (Refs. 5 and 6) proved to be an efficient transducer due to its extremely high sensitivity and a capability of detecting the motion of a mechanical resonator in the quantum limit. When capacitively coupled to the resonator and biased at a dc voltage, the SET senses the resonator's mechanical motion due to the variations in the electrical charge induced on the SET island. Using a radio frequency (rf) circuitry and an SET as a mixer, displacement sensitivity as good as 2×10^{-15} m/Hz^{1/2} was achieved for a GaAs mechanical resonator.⁷ In the later experiment, an rf version of the SET was used to detect the thermal motion of the SiN resonator demonstrating position resolution only a factor of 4.3 above the quantum limit.⁸

In this letter, we describe an aluminum structure that combines both the doubly clamped beam and SET, and therefore can be referred to as a two-in-one device. Our fabrication process allows easy integration of metallic nanomechanical resonators into the electronic circuits such as SETs or superconducting quantum interference devices. We show

experimentally that a conventional SET in the dc regime can detect flexural motion of its own island. We observe the frequency response of the suspended SET driven by an rf voltage applied to the bottom gate. The results are reproduced in the simulations based on the orthodox theory that takes into account the mechanical degree of freedom of the transistor. A similar device based on a carbon nanotube is reported in Refs. 9 and 10.

The device as well as wiring and voltage sources are shown schematically in Fig. 1. The central part of the SET is suspended above the substrate. It consists of an island connected to the source and drain electrodes through Al/AIO_x/Al tunnel junctions. There is a vacuum gap between the island as well as partly the source and drain electrodes and the bottom gate. Part of the island (shaded in Fig. 1) clamped between the source and drain electrodes can resonate. The suspension is made using the fabrication process described in Ref. 11. However, here we introduced one important modification. In addition to the regular side gate, an extra control electrode, called bottom gate, is placed underneath the island and partly under the source and drain electrodes. Such a multilayer two-gate configuration has certain advantages over the standard one-layer layout. First, the cou-

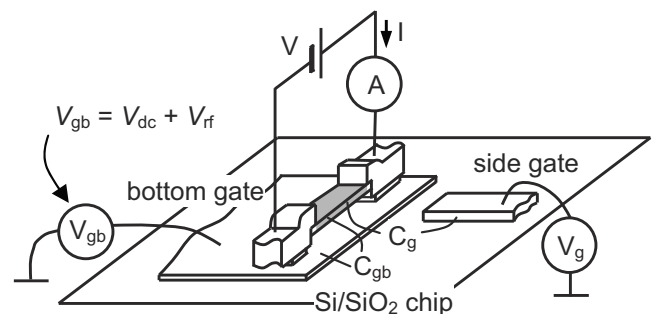


FIG. 1. Schematics of the suspended SET and measurement circuit.

^{a)}Electronic mail: pashkin@zp.jp.nec.com. On leave from P. N. Lebedev Physical Institute, Moscow 119991, Russia.

pling between the bottom gate and the island can be made several times larger as compared to the one-side gate configuration implemented in a single layer. This makes the SET more sensitive to mechanical motion. Second, the gap between the bottom gate and the island depends on the thickness of the corresponding polymer used as a sacrificial layer and therefore can be controlled accurately. Third, a high dc voltage V_{dc} and slowly varying voltage V_g can be applied to different gates simplifying the measurement process. The voltage applied to the bottom gate has following two components: $V_{gb} = V_{dc} + V_{rf}$. The former is used to control coupling between the mechanical motion and SET transport while the latter drives the beam. All the dc voltages are supplied to the sample by the filtered dc wires. The rf signal is delivered through a coaxial line with a 20 dB attenuator at 4.2 K. The measurements are done in a dilution refrigerator with a mixing chamber temperature of about 25 mK.

To model SET transport in the presence of mechanical oscillations, we perform simulations based on the orthodox theory¹² with the mechanical degree of freedom taken into account. We consider the classical dynamics of the SET island and solve the equation of motion for the coordinate x , which is the displacement of the beam center from the equilibrium position as follows:

$$\ddot{x} + \frac{\omega_0}{Q}\dot{x} + \omega_0^2 x = F/m, \quad (1)$$

where F is the driving force acting on the SET island, m is the beam effective mass, Q is the quality factor, and $\omega_0 = 2\pi f_0$ is the angular resonance frequency. The force can be found as a displacement derivative of the total energy stored in the SET island. Assuming $C_{gb} \ll C$, where C is the total capacitance of the SET island, we obtain $F \approx (\partial C_{gb} / \partial x) \times \{(1/2)V_{gb}^2 - (eV_{gb}/C)[n + (C_{gb}V_{gb}/e)]\}$, where n is the instant number of electrons on the SET island. We then further assume that the tunneling of electrons is much faster than the mechanical oscillations, so that the tunneling rate for each event can be calculated for constant x . The rates are calculated using the golden rule approach assuming both SET junctions are equal.

We first characterize the transistor by measuring the SET current I as a function of the bias voltage V and two following gate voltages: side gate voltage V_g and bottom gate voltage V_{dc} . From these measurements we estimate the following parameters of the device: total tunnel resistance $R = 140$ k Ω , charging energy $E_c = e^2/2C = 0.235$ meV ($E_c/k_B = 2.7$ K) corresponding to $C = 3.4 \times 10^{-16}$ F, and side gate capacitance $C_g = 1.2 \times 10^{-18}$ F. By sweeping the voltage applied to the bottom gate, we obtain its capacitance $C_{gb} = 5.4 \times 10^{-17}$ F. This value is in agreement with the naive estimation 2.4×10^{-17} F from the parallel-plate geometry, which underestimates the capacitance due to not taking into account the fringing effects as well as additional bottom gate–island coupling through the tunnel junctions. In this estimation, the island width $w = 92$ nm and length 1500 nm, and the vacuum ($\epsilon = 1$) gap $d = 50$ nm between the island and bottom gate, measured in the scanning electron microscope, were used. With the given dimensions of the 38.6-nm-thick island, and Al material parameters, such as the mass density 2700 kg/m³ and Young's modulus 70 GPa, we estimate the unstressed beam resonance frequency for the out-of-plane fundamental flexural mode to be about 90 MHz. However, as

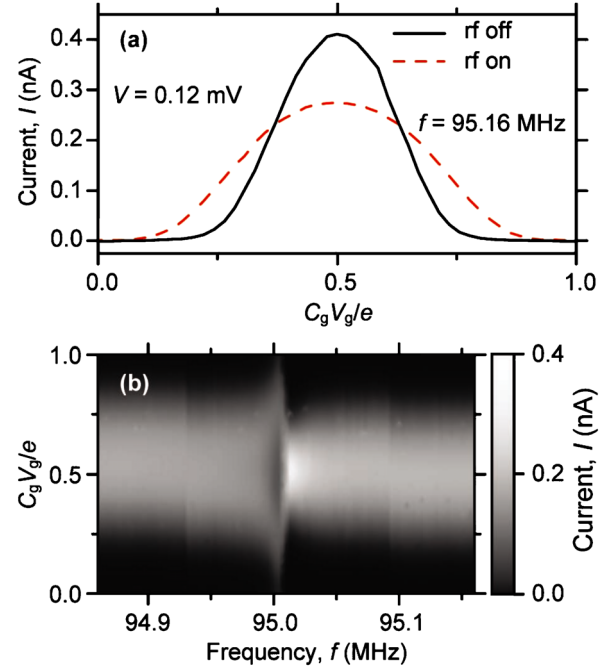


FIG. 2. (Color online) (a) I vs V_g curves for $V_{dc} = -2.5$ V and the amplitude of V_{rf} equal to 0 (solid curve) and 0.32 mV (dashed curve). (b) Intensity plot showing an SET modulation peak for the same values of V_{dc} and the amplitude of V_{rf} when the frequency of the applied drive is varied around resonance.

expected, the resonance frequency measured in the experiment is higher due to the tensile stress produced by the difference in thermal expansion coefficients of Al and Si.¹¹

In order to detect the beam resonance, we drive the beam with an external force by applying an rf voltage to the bottom gate inducing out-of-plane oscillations. To increase the coupling of the SET to the mechanical oscillations, we simultaneously apply to the same gate a high, up to ± 4 V, dc voltage. The search for the resonance is done in such a way that at fixed $V = 0.12$ mV and constant rf amplitude and frequency, we sweep V_g and measure current I through the SET. Then the frequency is increased by an increment of 3 kHz, which is smaller than the expected resonance width f_0/Q . Even in the absence of mechanical resonance the modulation peak gets slightly suppressed and broadened due to the fact that the working point shifts periodically when V_{rf} is applied [see Fig. 2(a)]. This effect, however, does not depend on frequency. Once the driving frequency approaches the resonance frequency of the beam, there is an additional effect on the modulation peak, which strongly depends on the frequency. The intensity plot revealing the expected resonance is presented in Fig. 2(b). The resonance is seen as a characteristic feature at about 95 MHz being most pronounced at $C_g V_g / e = 0.5$; the current peak height decreases first and then suddenly increases when we go through resonance from lower to higher frequency.

A collection of the SET response curves measured at various V_g and the corresponding simulated curves are shown in Fig. 3. In the simulations, we set $Q = 10^4$ and $f_0 = 95.007$ MHz; other parameters were taken from the experiment. Such a value of Q is consistent with those measured in our recent experiments on Al doubly clamped beams.¹³ The simulations capture all the essential features observed in the experiment. The current steps at about 94.93 and 95.09 MHz

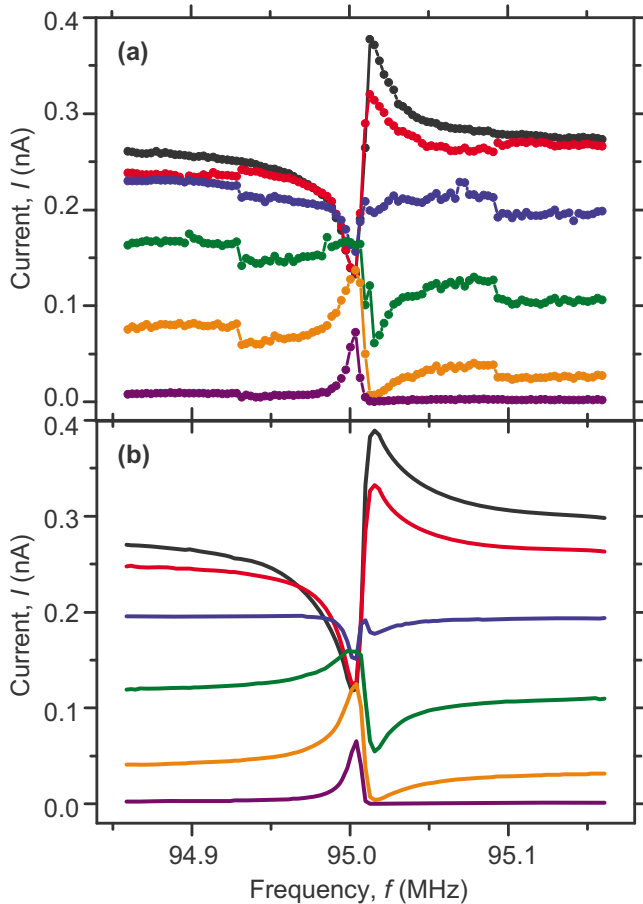


FIG. 3. (Color online) Frequency dependence of the SET current at $V_{dc} = -2.5$ V, amplitude 0.32 mV of V_{rf} and at several values of $C_g V_g / e$. (a) Response curves measured at $C_g V_g / e = 0.5, 0.42, 0.65, 0.77, 0.85,$ and 0.95 (from top to bottom). (b) Corresponding simulated curves.

in Fig. 3(a) are due to the jumps of the background charge, which were not accounted for in the simulations. Note that the observed response is expected in the fully linear regime; no nonlinearity of the resonator was included in the model. The observed dispersive-like resonance curve at $C_g V_g / e = 0.5$ instead of a Lorentzian expected for the driven harmonic oscillator in the linear regime can be qualitatively understood in the following way. When we approach the resonance from the lower frequency side, the SET modulation peak becomes more suppressed and smeared because both the driving force and the displacement effect act in phase. When we pass the resonance, the displacement and the driving force are shifted by 180° with respect to each other. Therefore they compensate each other, and the SET current rises to almost its original value when no rf voltage was applied. At a higher frequency, the amplitude of the

mechanical oscillations decreases and the modulation peak becomes almost equal to the one measured at a lower frequency.

The SET sensitivity to the mechanical motion can be estimated by setting the change in the island charge produced by the mechanical displacement equal to the SET charge equivalent noise. This gives the value $\delta x = q_n d / V_{dc} C_{gb} \approx 2 \times 10^{-13}$ m/Hz $^{1/2}$ per volt of V_{dc} assuming $x \ll d$ and taking a typical charge noise for Al SETs $q_n = 10^{-3}$ e/Hz $^{1/2}$ at 1 Hz.¹⁴ In fact, the displacement sensitivity is even lower due to rectification of the rf signal on the SET current nonlinearity. The rms amplitude of the beam main flexural mode due to thermal fluctuations is estimated from the equipartition theorem according to the formula $\langle x_T^2 \rangle^{1/2} = (k_B T / m \omega_0^2)^{1/2}$, where T is the temperature. This gives the value $\langle x_T^2 \rangle^{1/2} = 2.5 \times 10^{-13}$ m, which is not detectable in the present setup using dc measurement.

Besides detecting its own mechanical resonance, the device described can also be used for spectroscopy measurement of a suspended charge qubit. Another challenging experiment is the observation of the lasing effect in the circuit containing an artificial atom (charge qubit) coupled to a high-frequency mechanical resonator instead of a commonly used optical or microwave resonator.

We thank S. Asshab, N. Lambert, and F. Nori for fruitful discussions. This work was supported by the Funding Program for World-Leading Innovative R&D on Science and Technology (FIRST), CREST-JST, MEXT kakenhi “Quantum Cybernetics” and the Academy of Finland.

¹K. L. Ekinci and M. L. Roukes, *Rev. Sci. Instrum.* **76**, 061101 (2005).

²K. C. Schwab and M. L. Roukes, *Phys. Today* **58**, 36 (2005).

³X. M. H. Huang, C. A. Zorman, M. Mehregany, and M. L. Roukes, *Nature (London)* **421**, 496 (2003).

⁴M. Blencowe, *Phys. Rep.* **395**, 159 (2004).

⁵D. V. Averin and K. K. Likharev, *J. Low Temp. Phys.* **62**, 345 (1986).

⁶T. A. Fulton and G. J. Dolan, *Phys. Rev. Lett.* **59**, 109 (1987).

⁷R. G. Knobel and A. N. Cleland, *Nature (London)* **424**, 291 (2003).

⁸M. D. LaHaye, O. Buu, B. Camarota, and K. C. Schwab, *Science* **304**, 74 (2004).

⁹G. A. Steele, A. K. Hüttel, B. Witkamp, M. Poot, H. B. Meerwaldt, L. P. Kouwenhoven, and H. S. J. van der Zant, *Science* **325**, 1103 (2009).

¹⁰B. Lassagne, Y. Tarakanov, J. Kinaret, D. Garcia-Sanchez, and A. Bachtold, *Science* **325**, 1107 (2009).

¹¹T. F. Li, Yu. A. Pashkin, O. Astafiev, Y. Nakamura, J. S. Tsai, and H. Im, *Appl. Phys. Lett.* **92**, 043112 (2008).

¹²D. V. Averin and K. K. Likharev, *Mesoscopic Phenomena in Solids* (North-Holland, Amsterdam, 1991), pp. 173–271.

¹³F. Hoehne, Yu. A. Pashkin, O. Astafiev, L. Faoro, L. B. Ioffe, Y. Nakamura, and J. S. Tsai, *Phys. Rev. B* **81**, 184112 (2010).

¹⁴A. B. Zorin, F. J. Ahlers, J. Niemeyer, T. Weimann, H. Wolf, V. A. Krupenin, and S. V. Lotkhov, *Phys. Rev. B* **53**, 13682 (1996).